

Practical path planning techniques in overtaking for autonomous shuttles

Ehsan Malayjerdi¹  | Raivo Sell¹ | Mohsen Malayjerdi¹ | Andres Udal² |
Mauro Bellone³

¹Department of Mechanical and Industrial Engineering, Tallinn University of Technology, Tallinn, Estonia

²Department of Information Technology, Tallinn University of Technology, Tallinn, Estonia

³Smart City Center of Excellence, Tallinn University of Technology, Tallinn, Estonia

Correspondence

Ehsan Malayjerdi, Department of Mechanical and Industrial Engineering, Tallinn University of Technology, Ehitajate tee 5, Tallinn 19086, Estonia.

Email: ehsan.malayjerdi@taltech.ee and ehsan.malayjerdi@ttu.ee

Funding information

European Union's Horizon 2020 Research and Innovation Programme, Grant/Award Number: 856602; The European Regional Development Fund, co-funded by the Estonian Ministry of Education and Research, Grant/Award Number: 2014-2020.4.01.20-0289

Abstract

This paper proposes a reliable optimized sigmoid-based path planning algorithm that ensures smooth, fast and safe overtaking maneuver, while maintaining the necessary safety distance. In the proposed method, the desired smoothness of trajectories, the changes in steering angle and the lateral acceleration are controlled in a robust way. This paper describes the simulations, and the confirming real-world experiments, conducted using the autonomous shuttle iseAuto. Our results suggest that the sigmoid A-star algorithm leads to a smoother and more reliable motion when compared to other two standard methods. Specifically, the abruptness of necessary steering angle changes is reduced by factor of 4, and approaching the level of an experienced driver-like maneuver.

KEY WORDS

automated vehicle, optimization, path planning, trajectory evaluation

1 | INTRODUCTION

Self-driving vehicles and especially autonomous minibuses, also referred to as autonomous shuttles, are approaching exploitation in several cities worldwide. However, most of the autonomous shuttle projects are still in the test stage, and they can only demonstrate limited autonomous functionalities. One of the basic maneuver is to avoid collisions, for instance with a parked vehicle, by changing the driving lane. Although it may look a simple task to humans, most of the commercially available automation level 4 autonomous shuttles face difficulties in performing this task. Both research and manufacturers aim to bring the necessary improvements to vehicle safety, traffic accident rates, and vehicles' environmental impact. The first generation of autonomous shuttles could drive only in structured

environments with simple path planning algorithms. However, new self-driving vehicles in automation level 4 and 5 are expected to drive close to human drivers' basic skill (Committee et al., 2014), meaning that the self-driving algorithm must support more complex operations like lane-change, overtaking, etc.

In Hegeman et al. (2005) the authors argue that up to 10% of driving accidents are related to lane change events. It is clear that the lane change is not a safe maneuver even for human drivers, and lane changing to perform a safe overtaking is a tremendous challenge for automated shuttles. Overtaking algorithms require comprehensive information about the surrounding environment in all directions, and complex calculations of static and dynamic objects in the scene (Milanés et al., 2012). Furthermore, information about other problematic factors such as different weather conditions, various traffic

[Correction added on 20 January 2022, after first online publication: The original versions of Figures 15, 17, and 21 were from a prior version of the paper, and have now been updated to the final versions.]

situations, interaction with other road users (cars and pedestrians), and different road quality (C. Li, Wang, et al., 2015) are also required for the planning algorithm. As a result, path planning is considered as an essential subtask of the automated shuttles' software (Carroll et al., 1992; Chae & Yi, 2020; Majidi et al., 2017). It is typically divided into global and local path planners according to the planning scope (Lu et al., 2020). By considering the entire environment from the start point to the target point, global planners are primarily concentrated on generating a path that minimizes time and distance to reach the target. Local path planners, unlike the global ones, focus on improving driving safety, using sensory data and vehicle stability information, in the obstacle avoidance process by taking into account different constraints during the navigation.

With the final goal to improve urban maneuvers of autonomous shuttles, this paper describes a new approach for overtaking based on smooth sigmoid curves using a two-phase overtaking maneuver. The strategy stands on creating an optimized sigmoid function according to the shuttle kinematic model for fast, smooth and safe generation of overtaking paths based on perception, optimal low-level steering, and trajectory planning parameters. Figure 1 shows the two-phase of the overtaking maneuver: (I) lane change and obstacle passing, (II) return to the original lane and continuation. Furthermore, this paper introduces a high-fidelity simulation test bed to verify and validate algorithms performance before implementing on the real shuttle. An extensive experimental campaign was carried out using our automated shuttle—iseAuto (Rassölkön et al., 2018; Sell et al., 2018).

In summary, the main contributions of our work are: (1) A simple fast overtaking method able to take overtaking decisions and path planning within seconds; (2) A safe path planning approach that clearly shows the safe generated path using a verification procedure; (3) An improved human-machine interface by communicating the intention to overtake; (4) A safe overtaking method by generating a traffic-law compliant path that is verified in simulation and validated via implementation on a real automated shuttle demonstrating that the proposed method is safe and reliable.

The remainder of the paper is divided into eight sections: Section 2 presents related works on path planning algorithms that stand on Hybrid A-star, fuzzy logic, sigmoid functions or combination of different methods. Section 3 describes the kinematic model used for automated shuttles. Section 4 introduces our strategy for generating the sigmoid-based paths. Then the paper continues describing the simulation implemented in MatLab and the SVL environment. Our testbed vehicle is described in Section 6, including the sensor setup and the software

architecture. Section 7 proposes the experimental results on our test-site performed using different case study, including a comparison with other existing strategies, discussing their main limitations and our improved strategy. Relevant conclusions are drawn in Section 8.

2 | RELATED WORK

In self-driving vehicles, overtaking trajectories are computed in planning modules by decision-making algorithms. Different types of decision-making algorithms are available in the literature, such as binary decision diagrams (Claussmann et al., 2015), learning-based technologies (Liu et al., 2019, 2020; Mo et al., 2021) model predictive control (MPC), and nonlinear MPC (Palatti et al., 2021; Viana et al., 2019).

Planning modules are divided into path planning and trajectory planning. Path planning algorithms generate safe paths for obstacle avoidance based on vehicle dynamic (Wang et al., 2019), which represents an interesting topic for research in the field of self-driving vehicles. A wide range of algorithms have been used in related research including artificial potential fields method (APF) (Feng et al., 2021; Y. Huang, Ding, et al., 2019; Shufeng & Junxin, 2018; Wahid et al., 2020; Xie et al., 2021).

In Naranjo et al. (2008), a fuzzy logic controller is proposed for the lane change process. In this method, the fuzzy controller reacts as a driver behavior during the overtaking operation. Although the proposed method shows acceptable results in their three experiments, the information for navigation is fully based on GPS (Global Positioning System) data, thus resulting in possible lack of performance in case of signal loss of accuracy and reliability.

On a different line of research, the A-star as a graph search algorithm, and its improved variants, are widely studied and implemented (Dolgov et al., 2010; Montemerlo et al., 2008). However, the classical A-star algorithm has some limitation, such as path planning challenges on intersections (Erke et al., 2020), Shinpei, 2017, and computational time (Duchon et al., 2014). In this paper, some of these limitations are described and addressed in detail through some experiments. In Dixit et al. (2018), Lattarulo et al. (2017), the Bezier curves were utilized for the three-phase overtaking process through simulation. The proposed method has shown robust and smooth overtaking performance. However, the simulation was not reliable enough, and the method lacks of safety verification.

The method proposed in Chae and Yi (2020), Majidi et al. (2017) is an optimized global path planning algorithm with two-step optimization. Two cost functions were defined; first, minimizing the distance between the automated vehicle and the front vehicle at the starting point. Second, to minimize the sum of the automated vehicle lateral error from the reference path, and the steering velocity during the operation. Although the generated path was optimized, this study was carried out without any experiment and just based on a dynamic model in the CarSim simulator that is not realistic enough as a verification testbed.

In the field of path planning for autonomous driving, many research studies use mathematical functions such as quintic polynomial curves (Zhu et al., 2018), polynominal function (Chen & Huang, 2018),

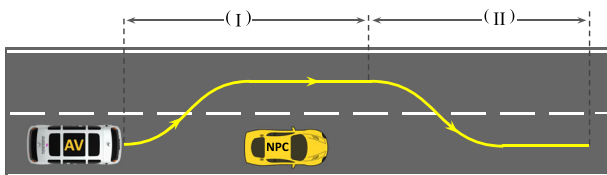


FIGURE 1 The overtaking maneuver by autonomous vehicle (AV) containing of the two lane change phases

Clothoid curves (Lambert et al., 2019; Liyang et al., 2020; Silva & Grassi, 2018), and sigmoid curve (Laghmara et al., 2019).

The sigmoid is a mathematical function which has a characteristic S-shape curve. Thanks to its nonlinearity, and the computational simplicity of its derivative, the sigmoid function is the most commonly used function in path planning. Of particular interest are the following three parameters: continuity, ease of discriminability, and simplicity (X. Li, Sun, et al., 2015), which constitute a motivation for using sigmoid functions for lane change maneuvers. A parameterized sigmoid based lane change operation is proposed in Ammour et al. (2020). In this method built for safe and comfortable lane change operation, the vehicle dynamics, and geometrical constraints, are considered in sigmoid functions for path planning. Ammour et al. create a path with a longitudinal distance, a lateral offset, and the trajectory curvature to develop a precise path tracking control strategy that minimizes the longitudinal and lateral error. Their simulation results show that the proposed algorithm has stable performance in lane change operation. A novel approach for obstacle avoidance on highway is proposed in Ammour et al. (2021), in their last method time-varied S-shaped sigmoid functions are used to define a restriction area based on the vehicle speed and distance to obstacles. The sigmoid S-shaped right side is an obstacle area, and the left side is defined as a safety gap for driving. Then the MPC algorithm is used for trajectory planning. The proposed method was only simulated in Matlab under three different scenarios. The simulation results show that this method has satisfactory results.

A Hybrid path planning algorithm is proposed in Lu et al. (2020), which combined Sigmoid curve with repulsive and attractive potential fields to improve performance, safety and feasibility of the generated paths. The overtaking path is created using the combination of obstacle avoidance, vehicle dynamics and sigmoid curves. The simulation results show that the proposed method improves vehicle stability and ride comfort during autonomous driving. An electronic driver assistance and collision avoidance system is proposed in Isermann et al. (2008). The system is a combination of object detection based on Lidar pointclouds fusion with camera images, path planning, and trajectory planning. The authors use the sigmoid curves for the path planning stage. The distance from front obstacles, safety area for lane change, and speed are the main parameters of their path planning algorithm. In the proposed system, the authors create the shortest evasive maneuver using sigmoid curves in consideration of the limitations of maximum lateral acceleration, maximum jerk, and dynamics of the steering actuator. Their experimental results and a comparison with klohoide functions show that the proposed method is able to provide a robust accident avoidance in Autonomous vehicles.

The method proposed in Ben-Messaoud et al. (2018) is a combination of parameterized sigmoid function and rolling horizon for generating a smooth path. The rolling horizon method is used for splitting the trajectory in convex areas. The authors argue that this method is effective in creating smooth and short overtaking paths. The rolling horizon method has been validated for lane changing process by simulation. The simulation results show that the algorithm effectively performs collision avoidance maneuvers for static and dynamic obstacles.

Supporting the use of sigmoid functions in generating paths, in X. Huang, Zhang, et al. (2019), it is used for creating overtaking maneuvers. The proposed method has shown successful overtaking in two simulated scenarios. In this method, the decision making is based on reference paths, distance between two vehicles, relative speed and safety factors. Experimental results show that the proposed method can properly handle the overtaking operation with a fixed velocity of the preceding vehicle.

Inspiring from previous literature and preserving our existing platform for autonomous driving, it became natural to implement a sigmoid A-star decision making algorithm as a combination of the Hybrid A-star and sigmoid functions to build fast, smooth, safe and reliable overtaking maneuvers. Differently with respect to previous literature describing the path planning with sigmoid function only in simulation, here an experimental evaluation using an autonomous shuttle in a urban environment is proposed.

3 | KINEMATIC MODEL OF AUTOMATED SHUTTLES

Figure 2 describes the simplified kinematic model of the automated shuttle with 3 degrees of freedom (x, y, φ). As most of the maneuvers considered in this study are taking place at a low speed below 15 km/h, it is estimated that the lateral accelerations of wheels remain below 0.2 g. As a result, the hypothesis of negligible sideslip of wheels can be applied (S. Li et al., 2019). That, in turn, makes it possible to perform trajectory calculations on the basis of kinematic model without considering more detailed effects present in sophisticated dynamical models. Thus the control task of the overtake maneuver can be simplified to the task of controlling changes in heading angle at a given speed according to the described kinematic model. Additionally, as the considered speed limit is relatively low in the present study (for safety reasons), only 1–2 s (1–4 m of distance) are used for the initial acceleration at the beginning of any maneuver, and most of the movements of automated shuttle will occur at a constant speed.

The steering model in Figure 2 describes the change of heading angle during time step dt at given velocity v , and current steering

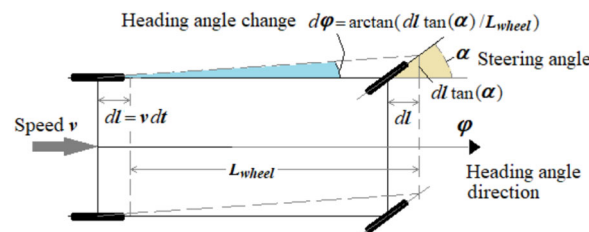


FIGURE 2 Kinematic model for the automated shuttle (“bicycle” model assumption). α denotes the steering angle of front wheels, φ is the heading angle of the vehicle, dl is the incremental forward displacement of rear wheels, $d\varphi$ is the resulting change of the heading angle, and finally L_{wheel} is the wheelbase

angle α . Possible sideslip corrections of the front wheels are omitted (S. Li et al., 2019), thus in a small time-step dt the rear wheels forward distance $dl = v \times dt$, while the movement of front wheels follows the steering angle α . As a result, incremental changes in the heading angle φ can be described by the following equation:

$$d\varphi = \arctan(dl \times \tan(\alpha)) / L_{wheel}. \quad (1)$$

Equation (1) can be simplified for small time-steps (small longitudinal movement steps dl) to:

$$d\varphi = dl \times \tan(\alpha) / L_{wheel} \quad (2)$$

and for modest steering angles ($|\alpha| \leq 0.1 \dots 0.2$ rad) further to:

$$d\varphi = dl \times \alpha / L_{wheel}. \quad (3)$$

Using Equation (3) it is possible to conclude that to achieve reasonable changes of heading angle (e.g., 0.3 rad, approximately 17°), the required driving distance should be of the order of the wheelbase L_{wheel} . As a result, the required minimum distance to perform full lane change maneuver should be of order of 2–3 wheelbases. The information about the wheelbase measure can be used to specify reasonable safety distances to avoid abrupt maneuvers.

4 | GENERATION OF SIGMOID PATHS FOR OVERTAKING

In this section, the motivation for moving from other standard methods, for instance the hybrid A-start algorithm, to the improved sigmoid-based path generation are explained. Then the sigmoid curve-based overtaking path generation algorithm is described in details.

4.1 | Limitations of the hybrid A-star algorithm

One of the challenges in the path planning for autonomous shuttle is to use a time varying input, for example, occupancy grid maps, required to create a path in dynamic environments, change as the vehicle moves. Hybrid A-star (Dolgov et al., 2010) is a modified A-star algorithm designed for autonomous vehicles path planning in dynamic areas, and implemented in our prototype (Rassölklin et al., 2018; Sell et al., 2018). First of all, the cost map, a fundamental concept in mobile robot navigation, is created from Lidar's data. Then,

this map is used to find efficient and safe routes across the point cloud map. A 2D cost map (gray rectangle) is shown in Figure 3. Black areas in the gray cost map represent objects in the map.

When the autonomous shuttle stops because of an obstacle on the waypoint, the Hybrid A-star algorithm starts iterating to find an alternative waypoint to avoid the obstacle. After generating a new path, the vehicle starts driving along the path. The Hybrid A-star, as a path planning algorithm for a mobile robot, was successfully implemented and tested. However, the results were not satisfactory and reliable. There are three important limitations using the Hybrid A-star for path planning on autonomous shuttles: (I) Computing time: the iterations to find an acceptable suboptimal trajectory is time-consuming. (II) Reliability: similarly to a random selection algorithm, there is no way to know that the generated path is the correct and safe for the operation; This is risky for an autonomous driving application with passengers (see Figure 4). (III) Lack of reactivity: the vehicle cannot react fast enough to a dynamically changing environment.

Therefore, further investigation was conducted to explore the possibilities of using the proposed sigmoid-based method to replace the Hybrid A-star.

4.2 | Overtaking using the sigmoid-based path

The decision making steps that lead to an overtaking operation are shown in Figure 5. The algorithm first checks for a probable detected object, if a static object is found in the detection range, then an overtaking maneuver should take place, consisting of a 3–5 s pause

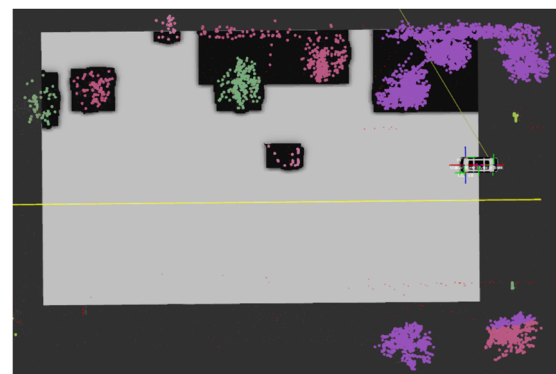


FIGURE 3 Cost map generated from the filtered 3D point cloud, the gray area corresponds to the drivable surface

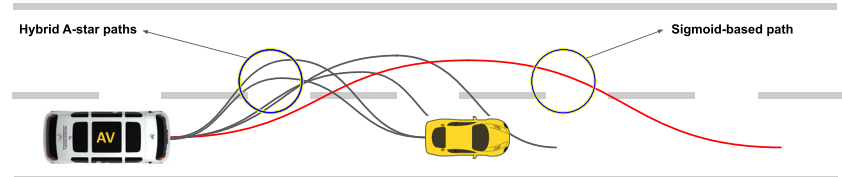


FIGURE 4 Comparison between the sigmoid-based and the Hybrid A-star generated path for overtaking

to prepare a new mission plan, then overtaking. In the case of the object restarting to move, the automated shuttle just decreases its speed and continues with the preset path generated using the A-star algorithm. In principle, this function pauses the trajectory following algorithm, that works on a pre-defined waypoint, and overlaps an optimized sigmoid-based generated path to overtake the obstacle, then resumes the original plan.

The first step in the overtaking maneuver is the detection of stationary objects that are blocking the initial desired waypoint path. Sometimes a vehicle might be blocking the entire road lane, but in many cases it could be blocking only part of it being parked on the roadside. If the object blocks the desired path, and it is in the detection range, the autonomous shuttle must stop. This is a safety requirement according to the current regulation, but in principle it is possible to overtake without a full stop. The detection range is approximately a rectangular area along the path with a predefined width, typically a little bit wider than the vehicle width (shown as green area in Figure 5).

In the implementation of the current overtaking algorithm, one of the main practical limitations is ensuring the smoothness of the steering angle changes maintaining the kinematic feasibility of the generated paths. This is necessary to ensure comfortable riding experience for passengers and to avoid a possible steering motor overload. In the case of overtaking maneuvers consisting of two lane changes (see Figure 6), one of the possible approaches to ensure a smooth turning and steering, is the application of two mathematically defined sigmoid functions.

In the field of automated shuttle control, only a few studies describe the application of sigmoid curves for the path planning, for example, Shao et al. (2018), S. Li et al. (2019), Lu et al. (2020). Our contribution along this line of research is the experimental report of a

practical application of this methodology proposed in literature only using simulations.

The first phase of the sigmoid path generation, referred to as STAGE I in Figure 6, can be described by the following Equation (4) including the exponential sigmoid term:

$$y_{\text{sig}1}(x) = y_0 - a(y_2 - y_0) + b \frac{(y_2 - y_0)}{1 + e^{\frac{x-x_0}{D_{01}}}}, \quad (4)$$

where y_0 is the initial y-coordinate of STAGE I starting point P_0 , y_2 is the desired final y-coordinate of STAGE I, the sigmoid center point x-coordinate x_0 is defined as the midpoint between P_1 and P_0 via $x_0 = \frac{x_1 + x_0}{2}$, and D_{01} is the abruptness parameter that is calculated as $1/k$ of the distance between the x-coordinates of the points P_1 and P_0 as $D_{01} = \frac{x_1 - x_0}{k}$. Offered factor $1/k$ defines what percentage of the lateral shift occurs in the "tail stabilization" area between the points $P_1 - P_2$, and the rest occurs between the points P_0 and P_1 . The fitting parameter values a and b are specified from the initial condition that the starting point of movement must coincide with P_0 , and the boundary value of y-coordinate must correlate with y-coordinate of the point P_2 .

Similarly, for sigmoid path in STAGE II, i.e. returning to the initial lane, a re-adaptation of Equation (4) can be used as follows:

$$y_{\text{sig}2}(x) = y_2 - a(y_4 - y_2) + b \frac{(y_4 - y_2)}{1 + e^{\frac{x-x_2}{D_{23}}}}, \quad (5)$$

where y_2 is the actual y-coordinate of STAGE II starting point (end-point of previous STAGE I), y_4 is the desired final y-coordinate of STAGE II, the sigmoid center point x-coordinate $x_2 = (x_2 + x_3)/2$ is defined as midpoint between P_2 and P_3 , and sigmoid abruptness parameter $D_{23} = (x_3 - x_2)/k$ is calculated by the difference of the x-coordinates of points P_3 and P_2 .

5 | OVERTAKING SIMULATIONS

This section contains the simulation setup that evaluates the sigmoid-based overtaking algorithm. First, the kinematic model and the sigmoid curve were implemented in MATLAB to tune the model by finding an optimized set of parameters to be validated in the SVL simulation environment, and finally used in the experimental setting.

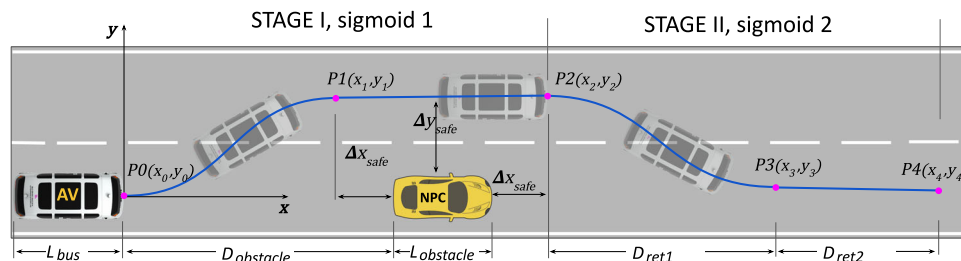


FIGURE 5 Five decision-making steps of the overtaking algorithm in the case an obstacle was detected by the shuttle

FIGURE 6 Overtaking maneuver description for a static obstacle. The two sigmoid paths are defined by the reference points $P_0 - P_1 - P_2$ and $P_2 - P_3 - P_4$, respectively

5.1 | Trajectory optimization

To evaluate the sigmoid curve utilization, and to achieve a comfortable ride with an accurate trajectory tracking (smooth steering), it is required to find the best parameter values for the sigmoid curve. Hence, the overtaking trajectory was simulated in a virtual model provided by MATLAB, and then a GA optimization algorithm (Wahde, 2008) was employed to find the best fit values. In the simulation, the "Vehicle Body 3DOF Dual Track" block as the automated vehicle kinematic model and the "Pure Pursuit" block to simulate the corresponding navigation controller were used.

The five main parameters were picked from the curve definition as follows: abruptness factor $k_{abruptness}$, distance to the obstacle D_{obs} , safety distance to the obstacle in the longitudinal direction Δx_{safe} , and the two longitudinal travel distances while returning to the driving lane D_{ret1}, D_{ret2} (see Figure 6). Moreover, the lookahead distance parameter $Lo_{distance}$ of the pure-pursuit controller was included to the optimization process to increase the trajectory following accuracy. The minimization of the following error leads to precise movement, which is required for maneuvers such as overtaking.

All the curve parameter values, and their descriptions are reported in Table 1 including their range of validity. After 500 simulation runs, GA found the optimum values reported in Table 2. For a better understanding of the optimization outcome, initial values were also suggested for the parameters listed in Table 2. Then, two simulations were performed by employing the initial and optimal data, while steering changes and trajectory tracking were recorded during the mission. Figure 7 shows the performance in tracking and steering by using suboptimal parameters and the optimized one. Figure 7a shows the not-optimized trajectory (red dots) and how the vehicle follows them (black circles), while Figure 7b shows the optimized trajectory. It is clear that the AV followed the optimized trajectory more accurately and also the steering changes are smoother (see Figure 8).

5.2 | SVL simulation

Several realistic car simulators are powered by a physics engine compatible with our automated shuttle control software, such as SVL and CARLA. They use modern game engine features like Unreal and

Unity, giving them the power to create complex virtual environments as well as realistic rendering.

In this paper, the SVL simulator (Rong et al., 2020) is used to assess the sigmoid-based overtaking algorithm. This simulator is based on the Unity game engine that provides various environments and car models in the simulation. For testing the maneuver in the simulator, a detailed iseAuto 3D model with the equipped Lidar was implemented inside Unity, and assigned the engine.

The evaluation process was built by creating a simple overtaking scenario inside the SVL simulator (see Figure 9). In this scenario, an NPC (Non-player character) car is placed in the middle of the waypoint, then the shuttle decision making capabilities are observed. Figure 9b reports the ROS visualization software screen that shows the point cloud of the simulated environment, the shuttle, and the vehicle's straight desired waypoint. In this figure, the shuttle detects an object in its waypoint's detection range (green area) and stops to take a decision on whether to perform an overtaking maneuver or not. The red line is visualized before the NPC as a stop indicator. Figure 9a shows the SVL simulation environment, including the iseAuto 3D model, and a stopped NPC. In the next step, the shuttle starts to generate a new smooth waypoint based on the sigmoid curve.

Figure 10 shows four time instants (frames) from start to end of the overtaking operation inside the simulator and the corresponding ROS visualization. Frame 1 shows that the new path, presented by Equation (1), is generated for STAGE I of overtaking Figure 10. Next, the shuttle starts to move toward the new waypoint (frame 2). After passing the object, the shuttle generates the new path starting the STAGE II of the mission using Equation (4). Finally, in the last frame, it returns to its original waypoint.

TABLE 2 Parameter values in a initial and optimized case

| Param. | Init. val. | Optim. val. | Param. | Init. val. | Optim. val. |
|------------------|------------|-------------|-------------------|------------|-------------|
| $Lo_{distance}$ | 5 m | 3.88 m | Δx_{safe} | 3 m | 3.49 m |
| $k_{abruptness}$ | 10 | 3.62 | $D_{ret.1}$ | 13 m | 13.04 m |
| $D_{obstacle}$ | 13 m | 14.28 m | $D_{ret.2}$ | 13 m | 10.93 m |

TABLE 1 Parameters for the kinematic model used in the optimization and experimental setup

| Param. | Val. | Description | Param. | Val. | Description |
|-------------------|---------|---------------------------|-------------------|--------|-------------------------------------|
| $D_{obstacle}$ | 8–15 m | Distance to obstacle | $L_{obstacle}$ | 4 m | Obstacle length in x-dir |
| W_{road} | 6 m | Road width | $W_{obstacle}$ | 2 m | Obstacle width in y-dir |
| Δx_{safe} | 3–5 m | Safety distance in x-dir. | $D_{ret.1\&2}$ | 5–15 m | Travel distance to the initial lane |
| L_{bus} | 3.4 m | Shuttle length | $Lo_{distance}$ | 3–8 m | Pure Pursuit Look-ahead distance |
| L_{wheel} | 2.55 m | Shuttle wheel base | Δy_{safe} | 2 m | Safety distance in y-dir |
| v | 10 km/h | Shuttle constant speed | $k_{abruptness}$ | 3–8 | abruptness factor |

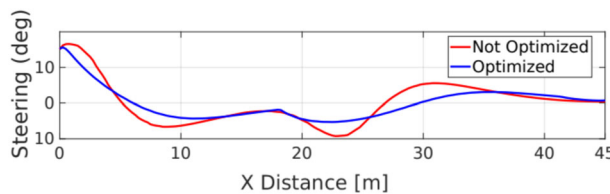
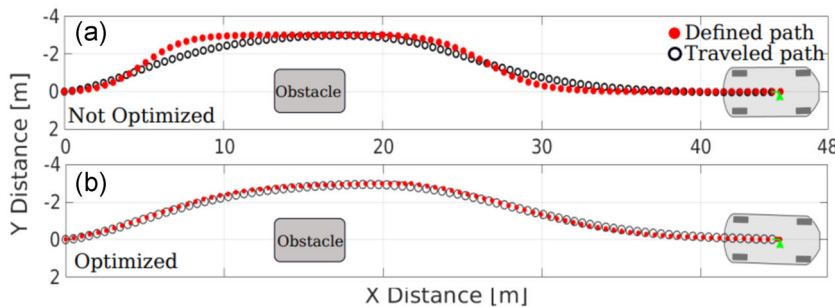


FIGURE 8 The comparison of and steering angle changes in the optimized and non-optimized case

6 | TESTBED

In this section, our customized automated vehicle and the testing environment are described.

6.1 | iseAuto automated shuttle

Our study was carried out by using the automated shuttle, iseAuto, at Tallinn University of Technology (TalTech), Estonia. The iseAuto is an automated shuttle belonging to the autonomous vehicles research group and operating in the campus for experimental and study purposes (see Figure 11). Previously proposed mechatronic design methodologies (Christophe et al., 2009; Sell et al., 2008) were implemented to focus on early design stages to develop the iseAuto shuttle from a scratch. The iseAuto project's objective was to build an open-source automated shuttle and establish a smart city testbed (Sell et al., 2020) in the TalTech campus. The further concept is to integrate an autonomous shuttle service with industrial parks as a part of Industry 4.0 concept (Sell et al., 2019). The automated shuttle and the testbed are connected to its digital twin, allowing designers to execute all development in simulation first. The simulation environments, interfaces, and concepts are described in detail in Medrano-Berumen et al. (2020), Malayjerdi et al. (2020).

The iseAuto high-level software architecture is based on ROS (Robotic Operating System). Perception, detection, and planning are performed by Autoware (Kato et al., 2018) an open-source ROS-based autonomous driving stack. Many advanced algorithms are already implemented, such as lane following, obstacle avoidance, traffic light detection, lane detection, etc. Lidars and

FIGURE 7 The comparison of trajectory following (a) not optimized case; (b) optimized case

Global Navigation Satellite System (GNSS) are used for localization and path following. The vehicle is equipped with two Velodyne Lidars at the top front (VLP-32) and top rear (VLP-16) of the vehicle, and two front sides Robosense RS-Bpearl to decrease blind spots. Furthermore, one RS-Lidars-16 is installed at the front bumper to detect small objects in front of the vehicle that are not in the other Lidars' field of view. Figure 12 shows the position of the Lidar sensors on the shuttle. Processes such as calibration, filtering, and concatenation were performed on the Lidars' point cloud to optimize perception capabilities.

The Lidars' raw point cloud is often noisy, contains outliers, and may cause errors in the detection process. Hence, it is essential to use a multi-step point-cloud filtering system that increases the perception algorithm performance and accuracy. First, ground filtering is applied to raw data to separate the ground points. Ring ground filter (Narksri et al., 2018) in Autoware is used as filtering method. This filter cuts unnecessary points, and avoids false detection of ground points as objects.

Next, from the Point Cloud Library (PCL), four different filtering methods are applied to filter the raw point cloud data: Voxel Grid, PassThrough, Statistical Outlier Removal and Radius Removal. Finally, the points are ready to be processed by the Euclidean clustering algorithm. These clustered points are used in the A-star algorithm to derive a grid map that is then used as a global scanning method to find an optimal path.

6.2 | Testsite experiment

After evaluating and verifying the new proposed method through simulation, as described in Section 5, the best found parameters were implemented on the iseAuto for testing a real scenario at the TalTech AV test site. The shuttle main processing unit is a PC with Ubuntu 18.04 operating system, AMD Ryzen threadripper 1950x, and two GeForce GTX-1080-Ti GPU. The experiments were conducted on a standard road with two lanes as shown in Figure 13. The shuttle speed was limited to 15 km/h (Figure 14).

7 | RESULTS AND DISCUSSION

To assess the performance of the maneuvers an extensive experimental campaign using the iseAuto automated shuttle was conducted. The steering angle feedback was recorded during the

FIGURE 9 (a) Simulation of an overtaking scenario in the SVL simulator. (b) The ROS visualization shows the vehicle sensor data, waypoint, and position in the map



FIGURE 10 Four characteristic time instants in SVL and the corresponding ROS simulation environment, describing the overtaking maneuver based on the smooth sigmoid-based path



FIGURE 11 TalTech iseAuto autonomous shuttle (left) and 3D eagle view map of the test site in TalTech campus (right)

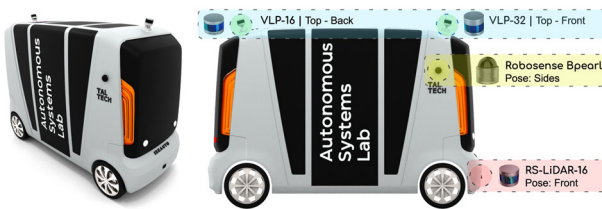


FIGURE 12 The iseAuto shuttle bus with the indication of the position of its three different types of Lidars



FIGURE 13 Automated shuttle iseAuto and a blue car stopped in the area where the experiments were carried out. Front view (a) and Drone view (b)

process both in simulation and experimental setup. The results show smoothness of the motion, efficiency and high reliability during the operation.

7.1 | Validation

To validate the optimized sigmoid-based paths, the results from the proposed method in simulation and in the experimental setup were recorded and reported in Figure 15b. The error between the simulation and the experiment is below 10% demonstrating the effectiveness of the method. Figure 15a shows the steering data for the two methods in simulation. The proposed optimized sigmoid-based method generates smoother steering angle changes than the guided Hybrid A-start, as the spikes visible on the blue-line at time 0 and 12 s were eliminated. Figure 15b shows the simulation result with the corresponding data from the experiment. Additionally, smooth trajectories yield to an improved use of the steering motors, since the angle range is reduced of about 5°. This reduces the long term usage of the motors, guarantees long-term steering motor performance and prevents unexpected failures.

This result validates the reliability of the experimental setup with respect to the simulation environment. In other words, the simulation of the overtaking maneuver presented in this paper shows that it is not essential to test newly developed algorithms directly on the automated shuttle; instead, they can be initially tested and verified

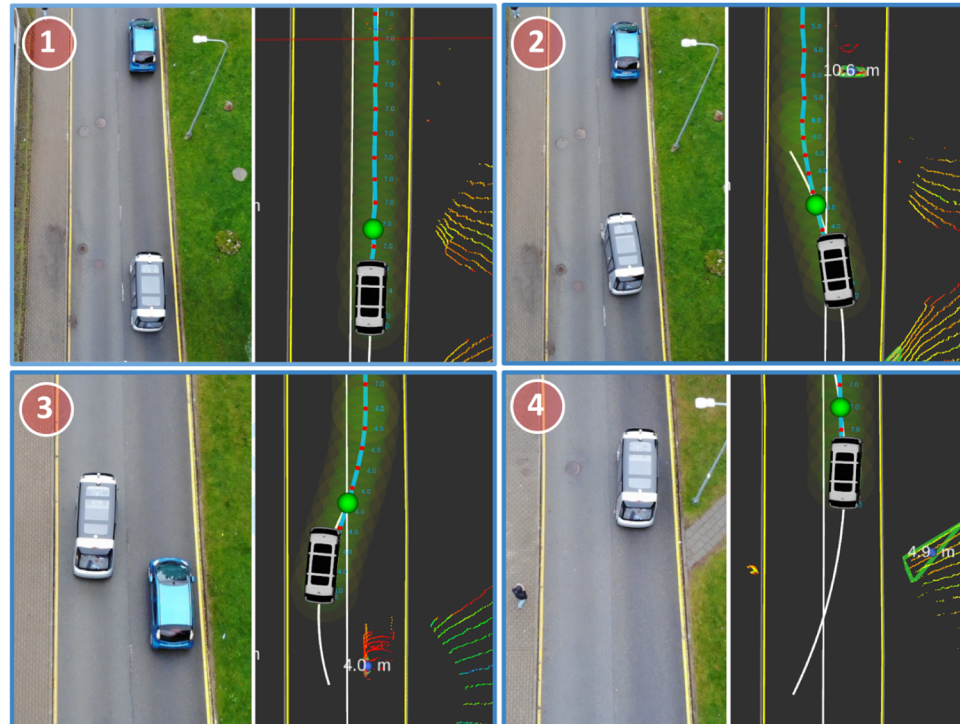


FIGURE 14 Different captured time frames of real overtaking experiment (drone view on left, ROS visualization on right)

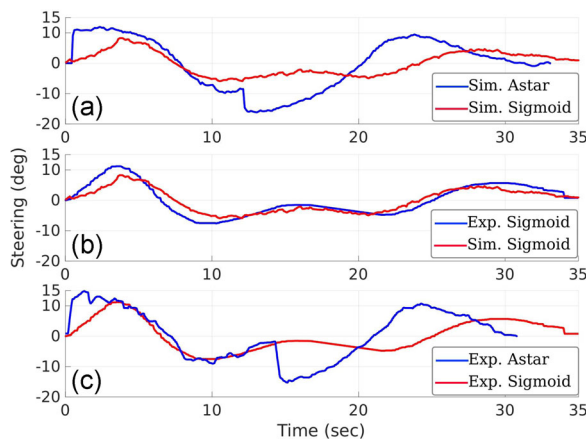


FIGURE 15 (a) Steering angle simulation data of the two different methods; guided Hybrid A-star and optimized Sigmoid. (b) Steering angle data of the simulation versus the experiment on sigmoid method. (c) Steering experiments data from the two methods

through the simulation platform. Although the stopped car scenario selected for the overtaking examination did not cover all the complex situations, it is an initial step for studying and introducing a verification platform for further research. Scenarios such as passing moving objects or vehicles coming from the opposite direction can be easily created and tested in the simulation without any danger.

7.2 | Experimental comparison

Similarly to the simulation environment, a long experimental campaign was conducted with both the sigmoid-based, the Hybrid A-star, and the Guided Hybrid A-star overtaking algorithm, while recording the steering data. In Figure 15c, the steering data of the sigmoid-based proposed method is compared against the corresponding data of the A-star-based method during the real experiments. As in Figure 15a, this plot also shows that the steering angle in the sigmoid-based path is smoother than the corresponding steering angle using the Guided Hybrid A-star method.

TABLE 3 Experimental results reported from four case studies that were carried out with three different methods

| Method | Parameter | Case(a) | Case(b) | Case(c) | Case(d) |
|-------------------------|---------------------------|-------------|-------------|-------------|-------------|
| Hybrid A-star | Duration(s) | NA | NA | NA | NA |
| | Computational time (s) | 77.36 | 36.56 | 159.32 | 112.51 |
| | Maximum wheel angle (rad) | 0.22 | 0.36 | 0.35 | 0.32 |
| | Path length (m) | 29.62 | 31.05 | 39.06 | 44.88 |
| | Number of iterations | 154 | 72 | 318 | 224 |
| | Created path | 3 | 3 | 13 | 8 |
| Guided Hybrid A-star | Overtaking result | Failed | Failed | Failed | Failed |
| | Duration (s) | 23.36 | 25.80 | 33.90 | 39.30 |
| | Computation time (s) | 10 | 10 | 10 | 10 |
| | Maximum wheel angle (rad) | 0.31 | 0.36 | 0.35 | 0.32 |
| | Path length (m) | 29.62 | 31.05 | 39.06 | 44.88 |
| | Number of iterations | 1 | 1 | 2 | 3 |
| Optimized Sigmoid curve | Created path | 2 | 2 | 2 | 2 |
| | Overtaking result | Pass | Pass | Pass | Pass |
| | Duration | 25.23 | 28.32 | 39.40 | 45.60 |
| | Computation time (s) | 10 | 10 | 10 | 10 |
| | Maximum wheel angle (rad) | 0.28 | 0.30 | 0.29 | 0.30 |
| | Path length (m) | 40.23 | 45.36 | 53.42 | 61.34 |
| | Number of iterations | 2 | 2 | 3 | 4 |
| | Created path | 2 | 2 | 3 | 4 |
| | Overtaking result | Pass | Pass | Pass | Pass |
| | | | | | |

Note: Bold values indicate the smoothening efficiency of the optimized sigmoid method.

7.3 | Case study

To further demonstrate the effectiveness of the proposed method, four different case study have been proposed in simulation and experimental setup. In the experimental setup the trajectory driven by the vehicle was recorded using a drone from the top view (see Figure 13a). The results are shown in Table 3.

7.3.1 | Overtake using guided lane change

In the first experiment an alternative waypoint was created manually on the opposite lane. Such waypoint is generated as a safe path for the lane change process during the overtaking maneuver. Figure 16 shows the two waypoints, in each figure the bold blue line represents the original path, and the dash line at the vehicle left side is the alternative one. As shown in Figure 16a, the green ball, which is the local control goal, is on the original waypoint. When the autonomous shuttle detects an obstacle on the path, the alternative path changes to the main path. As seen in Figure 16b, the green ball suddenly switched to the alternative waypoint that causes a rough and sharp motion for lane changing Figure 16c. Then the same lane change happens when driving back to the original path after passing the obstacle. In Figure 16d the original waypoint is enabled so the green ball jumps on it. As seen in Figure 16e cause the same issue that happened on 16c. This fast switch between routes might cause safety issues for passengers and technical problems for the steering mechanism due to its restriction. To solve this issue, in another test, the Hybrid A-star algorithm was used for overtaking the same scenario.

7.3.2 | Overtake with Hybrid A-star path planning algorithm

In the second experiment, the Hybrid A-star algorithm is customized for automated shuttle overtaking (Figure 17). As shown in Figure 17a–e, the Hybrid A-star algorithm generated different paths in different time-stamps. As seen in Figure 17a when the autonomous shuttle detects an obstacle on its waypoint, the Hybrid A-star creates a path for obstacle avoidance. Then the shuttle starts driving on the newly generated path. As shown in Figure 17b at 6 m from the obstacle, suddenly the Hybrid A-star updates its path close to the obstacle resulting in an unexpected shuttle hard brake due to safety range sensors detecting an obstacle in the close range. In the next iteration, (see Figure 17c) the Hybrid A-star generates a new avoiding path. Following the generated path, and once the obstacle is overtaken, the Hybrid A-star updates its path once more (see Figure 17d). At this point there is a conflict of different generated paths as the shuttle attempts to turn right but the Hybrid A-star updates its waypoint again 17e.

Based on the experimental result, the Hybrid A-star algorithm cannot be considered safe and reliable for the application in our vehicle. In the next experiment, the guided Hybrid A-star algorithm performance is evaluated.

7.3.3 | Overtake with the guided Hybrid A-star

In this section, the guided Hybrid A-star algorithm performance is described from a practical overtaking operation point of view (Figure 18). In this method, four safe points are defined for two



FIGURE 16 Guided lane change algorithm in the first overtaking experiment: (a) initial obstacle detecting situation; (b) switching the trajectory to the alternative waypoint for avoiding the obstacle; (c) driving at maximum speed and steering angle to reach the new waypoint; (d) switching the trajectory to the original waypoint after passing the obstacle. (e) driving at maximum speed and steering angle to reach the original waypoint

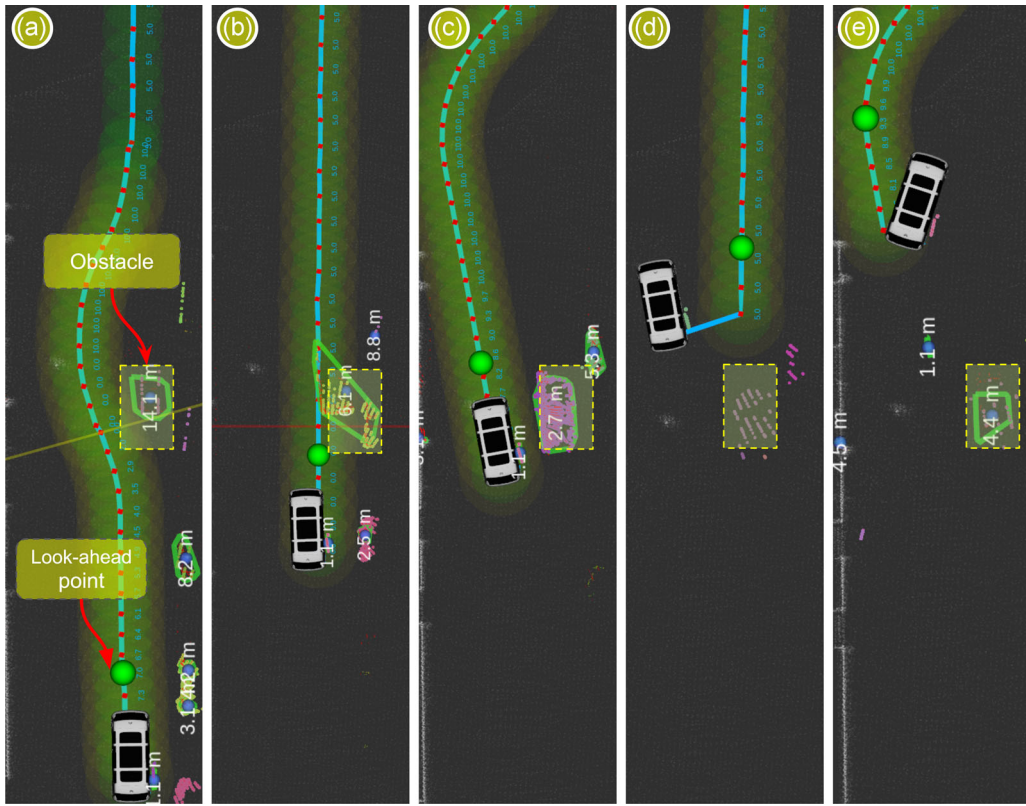


FIGURE 17 Hybrid A-star iterations for the overtaking maneuver in the test-bed experiment; (a) obstacle detection at 14.2 m and creating a avoidance path; (b) change of the avoidance path to a straight path at 5.8 m from the obstacle; (c) an additional avoidance path is created; (d) while driving on the previous path, the next iteration creates a new path; (e) the autonomous shuttle attempts to drive on the generated path with previous iteration, suddenly the iteration generates a conflicting path choice

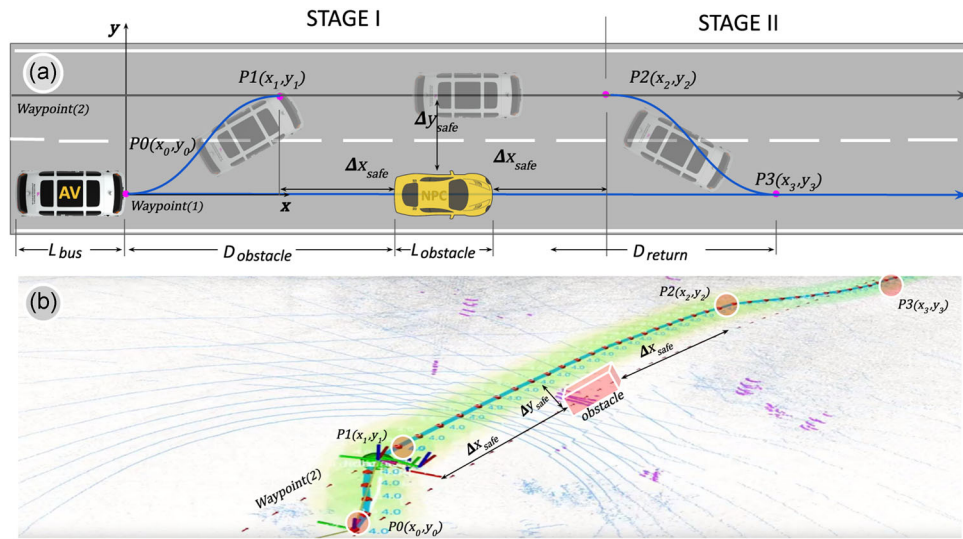


FIGURE 18 Overtaking maneuver description with the guided Hybrid A-star method. Four references points P_0 , P_1 , P_2 , P_3 are defined for Hybrid A-star to create a path (a). ROS visualization from experiment (b)

overtaking stages. P_0 is the safety distance between the automated shuttle and the obstacle. P_1 is the goal for the Hybrid A-star to create a smooth path from P_0 to P_1 . The P_1 point is based on the safety distance from the obstacle in the longitudinal direction Δx_{safe} and

lateral direction Δy_{safe} . When the automated shuttle reaches the point P_1 , driving on a straight line toward the next predefined point P_2 . Also this point is based on Δx_{safe} and Δy_{safe} . Then P_2 is set as the starting point for the Hybrid A-star, and P_3 as the end point to create a path.

The point P_3 is on the main waypoint and fulfils the safety distance requirement from the obstacle.

An additional experiment is shown in Figure 18b, here the automated shuttle calculates the car length. Based on the vehicle length, the algorithm calculates the position of the points P_1 , P_2 , and P_3 , and finally the automated shuttle drives on the overtaking path. Reliability and safety issues in the Hybrid A-star algorithm are solved with this method. However, there are two big drawbacks. First, the automated shuttle still requires the second predefined waypoint for choosing the points P_1 , P_2 . Second, the automated shuttle must run the Hybrid A-star algorithm twice, one for each overtaking stage.

7.3.4 | Overtake using the optimized sigmoid-based method

The performance of the proposed sigmoid-based method is described using four practical overtaking operations (see Figure 19).

Case study (a): In this case study, similarly to the simulation environment, the experiment is illustrated by using different time frames in which the first is the top view captured by a drone (see Figure 14). The second is the corresponding screenshot from the ROS visualization software, which shows the pre-designed waypoint and the current shuttle position. Figure 14 (frame 1) shows that the automated shuttle correctly detected the vehicle and indicated using a red line in the ROS visualization. Hence, the automated shuttle should stop. Clearly, the obstacle vehicle is not shown in the ROS visualization because the pre-defined path could not predict the presence of the vehicle, demonstrating the high

adaptive capability to this dynamically changing environment. When the shuttle stops, the overtaking operation can begin, and the new waypoint is generated (frame 2). Observe that Figure 14 (frame 2) also includes an indication of the distance between the automated shuttle and the obstacle in the ROS visualization. Frame 3 shows that the vehicle passed the car and started to return to its original lane or waypoint, also in this case the frame includes an indication of the longitudinal distance between the automated shuttle and the overtaken obstacle. Finally, the last frame shows that the shuttle is back to the original lane and continues its mission.

Case study (b): During the initial stage of an overtaking maneuver, it is very hard to calculate the total path length as the length of the obstacle is not known a-priori and thus there is no guarantee about the total duration of the maneuver. In this case a perception algorithm using the right-side Lidar data, is added to proposed method as an additional decision making step (see Figure 20).

The 3D overtaking area in Figure 20(1) is created at the autonomous shuttle right side. The length, in this case, is 16 m (covering 6 m from the back side to 10 m on the front side), the height and depth are 2 m. Also the Yolov3, a real time object detection system (Redmon & Farhadi, 2018) that uses the autonomous shuttle right camera is combined with the lidar perception. This perception algorithm is implemented as a service, and it runs for overtaking maneuvers. At the beginning of the STAGE I, the perception service is called by the overtaking algorithm. When the autonomous shuttle is at the



FIGURE 19 Different scenarios for overtaking. Overtake from a long vehicle (a), Overtake from a long and small vehicle (b). Overtake from a long vehicle and two small vehicle (c)

second lane, before going to STAGE II, the service calculates the overtaken vehicle length and check the 3D dimensional box (Figure 20(1)) for lane change permission. If the overtaking area is free, the overtaking algorithm uses the obstacle length to initiate the STAGE II starting at a safety distance from the overtaken obstacle.

Case study (c): In this experiment the automated shuttle overtakes two vehicles. As seen in Figure 21b, the performance of proposed method for overtaking is tested in different scenarios. In this case, the autonomous shuttle calls the perception service, then the service calculates the length of the overtaken obstacle and detects another vehicle on the road, see Figure 20(3). As a consequence, the overtaking algorithm does not have the lane change back permission and continues driving until permission as in Figure 21(b). Once the vehicle has the permission, the second STAGE II makes

a path for lane change back at the safe distance from the second vehicle position.

Case study (d): In this experiment, the performance of the perception algorithm is tested to overtake three cars on the road. In this scenario, after passing the second car, another car detected by perception algorithm. So the autonomous shuttle continues driving until permission. Once the vehicle has the permission, make a lane change back for returning to the main lane. As seen in (see Figure 21c) the automated shuttle overtakes three cars successfully.

8 | CONCLUSION

In this paper, an optimized sigmoid-based overtaking maneuver generator for an autonomous shuttle is experimentally studied. To overcome the limitation of the current state-of-the-art algorithms, a modified path planning algorithm based on the sigmoid curve is proposed.

Smoothness, safety, and reliability were the main criteria for the automated shuttle overtaking process that were in the core values of our design. The proposed overtaking algorithm has been developed, formulated and implemented on a real automated shuttle, and experiments were conducted on real road scenarios. The proposed methodology for overtaking from one vehicle can be extended to overtaking multiple vehicles. High-fidelity simulations were used to validate the efficiency and to predict the behavior of the proposed algorithm. The results showed that the proposed method efficiently reduced the steering effort and removed sharp changes that led to uncomfortable and unsafe operations. According to our experimental results, the proposed method over performs other state of the art methods, specifically the Hybrid A-star and the guided Hybrid A-star.

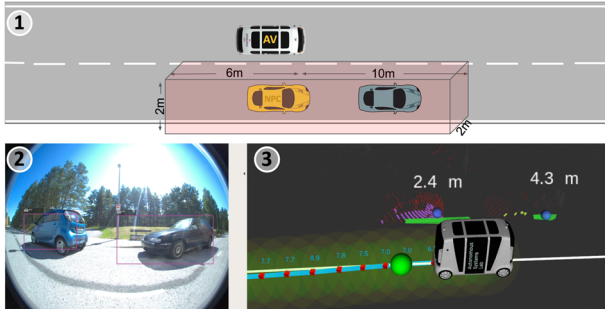


FIGURE 20 Perception algorithm using the right-side lidar data. (1) The top-view of the bus in which the obstacle box is shown. (2) Right side camera view. (3) ROS visualization of the vehicle path

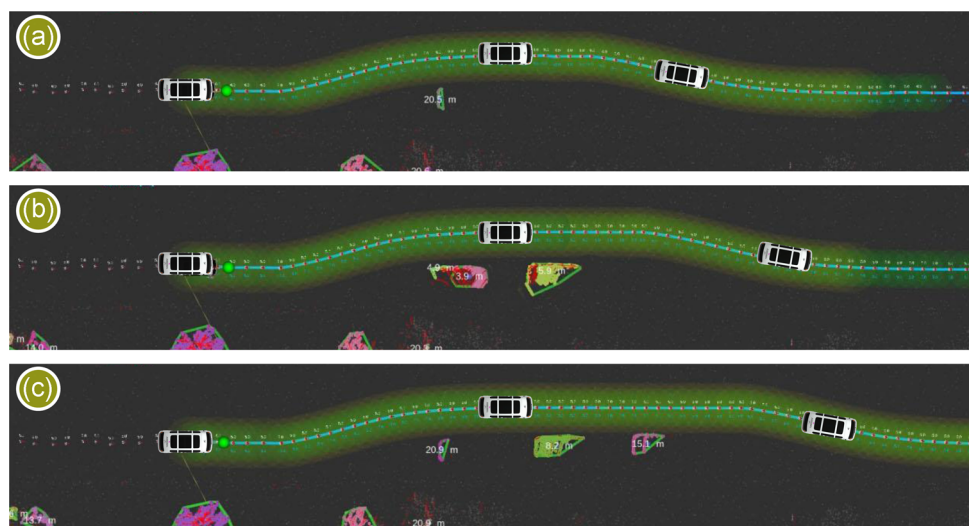


FIGURE 21 Different scenarios of real overtaking experiment with proposed method in the ROS visualization environment. (a) Overtake a long vehicle; (b) overtake a long and small vehicle case; (c) overtake a long vehicle and two small vehicle

Future investigations are required to focus on advanced obstacle avoidance methods drawn from this study for complex scenarios such as moving vehicles, extend and improve perception for fast and precise detection, and overtaking with high speed. It is required to use the developed method for movement prediction in this regard. Furthermore, an extra decision-making step should be added to the algorithm based on information from the camera image and machine learning algorithms.

ACKNOWLEDGMENTS

The author(s) disclosed receipt of the following financial support for the research, authorship, and/or publication of this article: This study has received funding from two grants: the European Union's Horizon 2020 Research and Innovation Programme, under the grant agreement No. 856602, and the European Regional Development Fund, co-funded by the Estonian Ministry of Education and Research, under grant agreement No 2014-2020.4.01.20-0289.

CONFLICT OF INTERESTS

The authors declare that there are no conflict of interests.

DATA AVAILABILITY STATEMENT

The data that support the findings of this study are available from the corresponding author upon reasonable request.

ORCID

Ehsan Malayjerdi  <http://orcid.org/0000-0002-6526-6059>

REFERENCES

- Ammour, M., Orjuela, R. & Basset, M. (2020) Trajectory reference generation and guidance control for autonomous vehicle lane change maneuver. In *2020 28th Mediterranean Conference on Control and Automation (MED)* (pp. 13–18). Saint-Raphaël, France: IEEE 2020 28th Mediterranean Conference on Control and Automation (MED).
- Ammour, M., Orjuela, R. & Basset, M. (2021) Collision avoidance for autonomous vehicle using MPC and time varying sigmoid safety constraints. *IFAC-PapersOnLine*, 54(10), 39–44.
- Ben-Messaoud, W., Basset, M., Lauffenburger, J.-P. & Orjuela, R. (2018) Smooth obstacle avoidance path planning for autonomous vehicles. In *2018 IEEE International Conference on Vehicular Electronics and Safety (ICVES)* (pp. 1–6). Madrid, Spain: IEEE.
- Carroll, K. P., McClaran, S. R., Nelson, E. L., Barnett, D. M., Friesen, D. K. & William, G. N. (1992) Auv path planning: an a* approach to path planning with consideration of variable vehicle speeds and multiple, overlapping, time-dependent exclusion zones. In *Proceedings of the 1992 Symposium on Autonomous Underwater Vehicle Technology* (pp. 79–84). Washington, DC, USA: IEEE.
- Chae, H. & Yi, K. (2020) Virtual target-based overtaking decision, motion planning, and control of autonomous vehicles. *IEEE Access*, 8, 51363–51376.
- Chen, Y. & Huang, Y. (2018) An overtaking obstacle algorithm for autonomous driving based on dynamic trajectory planning. In *2018 14th International Conference on Natural Computation, Fuzzy Systems and Knowledge Discovery (ICNC-FSKD)* (pp. 1315–1322). Huangshan, China: IEEE.
- Christophe, F., Sell, R., Bernard, A. & Coatanéa, E. (2009) Opas: ontology processing for assisted synthesis of conceptual design solutions. In *International Design Engineering Technical Conferences and Computers and Information in Engineering Conference* (Vol. 49026, pp. 249–260). San Diego, California, USA: ASME.
- Claussmann, L., Carvalho, A. & Schildbach, G. (2015) A path planner for autonomous driving on highways using a human mimicry approach with binary decision diagrams. In *2015 European Control Conference (ECC)* (pp. 2976–2982). Linz, Austria: IEEE.
- Dixit, S., Fallah, S., Montanaro, U., Dianati, M., Stevens, A., McCullough, F. & Mouzakitis, A. (2018) Trajectory planning and tracking for autonomous overtaking: state-of-the-art and future prospects. *Annual Reviews in Control*, 45, 76–86.
- Dolgov, D., Thrun, S., Montemerlo, M. & Diebel, J. (2010) Path planning for autonomous vehicles in unknown semi-structured environments. *The International Journal of Robotics Research*, 29(5), 485–501.
- Duchoň, F., Babinec, A., Kajan, M., Beňo, P., Florek, M., Fico, T. & Jurišica, L. (2014) Path planning with modified a star algorithm for a mobile robot. *Procedia Engineering*, 96, 59–69.
- Erke, S., Bin, D., Yiming, N., Qi, Z., Liang, X. & Dawei, Z. (2020) An improved a-star based path planning algorithm for autonomous land vehicles. *International Journal of Advanced Robotic Systems*, 17(5), 1729881420962263.
- Feng, S., Qian, Y. & Wang, Y. (2021) Collision avoidance method of autonomous vehicle based on improved artificial potential field algorithm. *Proceedings of the Institution of Mechanical Engineers, Part D: Journal of Automobile Engineering*, 235(14), 3416–3430.
- Hegeman, G., Brookhuis, K. & Hoogendoorn, S. (2005) Opportunities of advanced driver assistance systems towards overtaking. *European Journal of Transport and Infrastructure Research*, 5(4).
- Huang, X., Zhang, W. & Li, P. (2019) A path planning method for vehicle overtaking maneuver using sigmoid functions. *IFAC-PapersOnLine*, 52(8), 422–427.
- Huang, Y., Ding, H., Zhang, Y., Wang, H., Cao, D., Xu, N. & Hu, C. (2019) A motion planning and tracking framework for autonomous vehicles based on artificial potential field elaborated resistance network approach. *IEEE Transactions on Industrial Electronics*, 67(2), 1376–1386.
- Isermann, R., Schorn, M. & Stählin, U. (2008) Anticollision system Proreta with automatic braking and steering. *Vehicle System Dynamics*, 46(S1), 683–694.
- Kato, S., Tokunaga, S., Maruyama, Y., Maeda, S., Hirabayashi, M. & Kitsukawa, Y. (2018) Autoware on board: Enabling autonomous vehicles with embedded systems. In *2018 ACM/IEEE 9th International Conference on Cyber-Physical Systems (ICCPS)* (pp. 287–296). Porto, Portugal: IEEE.
- Laghmara, H., Boudali, M.-T., Laurain, T., Ledy, J., Orjuela, R., Lauffenburger, J.-P. & Basset, M. (2019) Obstacle avoidance, path planning and control for autonomous vehicles. In *2019 IEEE Intelligent Vehicles Symposium (IV)* (pp. 529–534). Paris, France: IEEE.
- Lambert, E., Romano, R. & Watling, D. (2019) Optimal path planning with clothoid curves for passenger comfort. In *Proceedings of the 5th International Conference on Vehicle Technology and Intelligent Transport Systems (VEHITS 2019)* (Vol. 1, pp. 609–615). SciTePress.
- Lattarulo, R., Marcano, M. & Pérez, J. (2017) Overtaking maneuver for automated driving using virtual environments. In *International Conference on Computer Aided Systems Theory* (pp. 446–453). Springer.
- Li, C., Wang, J., Wang, X. & Zhang, Y. (2015) A model based path planning algorithm for self-driving cars in dynamic environment. In *2015 Chinese Automation Congress (CAC)* (pp. 1123–1128). IEEE.
- Li, S., Li, Z., Yu, Z., Zhang, B. & Zhang, N. (2019) Dynamic trajectory planning and tracking for autonomous vehicle with obstacle avoidance based on model predictive control. *IEEE Access*, 7, 132074–132086.
- Li, X., Sun, Z., Cao, D., He, Z. & Zhu, Q. (2015) Real-time trajectory planning for autonomous urban driving: framework, algorithms, and verifications. *IEEE/ASME Transactions on Mechatronics*, 21(2), 740–753.

- Liu, T., Deng, Z., Tang, X., Wang, H. & Cao, D. (2019) Predictive freeway overtaking strategy for automated vehicles using deep reinforcement learning. In *2019 3rd Conference on Vehicle Control and Intelligence (CVCI)* (pp. 1–6). Hefei, China: IEEE.
- Liu, T., Huang, B., Deng, Z., Wang, H., Tang, X., Wang, X. & Cao, D. (2020) Heuristics-oriented overtaking decision making for autonomous vehicles using reinforcement learning. *IET Electrical Systems in Transportation*, 10(4), 417–424.
- Liyang, S., Yu, H., Xuezhi, C., Changhao, J. & Miaohua, H. (2020) Path planning based on clothoid for autonomous valet parking. In *2020 17th International Computer Conference on Wavelet Active Media Technology and Information Processing (ICCWAMTIP)* (pp. 389–393). Chengdu, China: IEEE.
- Lu, B., He, H., Yu, H., Wang, H., Li, G., Shi, M. & Cao, D. (2020) Hybrid path planning combining potential field with sigmoid curve for autonomous driving. *Sensors*, 20(24), 7197.
- Majidi, M., Arab, M. & Tavoosi, V. (2017) *Optimal real-time trajectory planning of autonomous ground vehicles for overtaking moving obstacles*. Technical report, SAE Technical Paper.
- Malayjerdi, M., Kuts, V., Sell, R., Otto, T. & Baykara, B. C. (2020) Virtual simulations environment development for autonomous vehicles interaction. In *IMECE2020*. ASME.
- Medrano-Berumen, C., Malayjerdi, M., Akbaş, M. İ., Sell, R. & Razdan, R. (2020) Development of a validation regime for an autonomous campus shuttle. In *2020 SoutheastCon* (pp. 1–8). IEEE.
- Milanés, V., Llorca, D. F., Villagrá, J., Pérez, J., Fernández, C., Parra, I., González, C. & Sotelo, M. A. (2012) Intelligent automatic overtaking system using vision for vehicle detection. *Expert Systems with Applications*, 39(3), 3362–3373.
- Mo, S., Pei, X. & Wu, C. (2021) Safe reinforcement learning for autonomous vehicle using Monte Carlo tree search. *IEEE Transactions on Intelligent Transportation Systems*.
- Montemerlo, M., Becker, J., Bhat, S., Dahlkamp, H., Dolgov, D. & Ettinger, S. (2008) Junior: the Stanford entry in the urban challenge. *Journal of Field Robotics*, 25(9), 569–597.
- Naranjo, J. E., Gonzalez, C., Garcia, R. & De Pedro, T. (2008) Lane-change fuzzy control in autonomous vehicles for the overtaking maneuver. *IEEE Transactions on Intelligent Transportation Systems*, 9(3), 438–450.
- Narksri, P., Takeuchi, E., Ninomiya, Y., Morales, Y., Akai, N. & Kawaguchi, N. (2018) A slope-robust cascaded ground segmentation in 3d point cloud for autonomous vehicles. In *2018 21st International Conference on intelligent transportation systems (ITSC)* (pp. 497–504). IEEE.
- Palatti, J., Aksjonov, A., Alcan, G. & Kyrki, V. (2021) Planning for safe abortable overtaking maneuvers in autonomous driving. *arXiv preprint arXiv:2104.00077*.
- Rassölklin, A., Sell, R. & Leier, M. (2018) Development case study of the first Estonian self-driving car, iseauto. *Electrical, Control and Communication Engineering*, 14(1), 81–88.
- Redmon, J. & Farhadi, A. (2018) Yolov3: an incremental improvement. *arXiv*.
- Rong, G., Shin, B. H., Tabatabaei, H., Lu, Q., Lemke, S. & Možeiko, M. (2020) Lgsvl simulator: a high fidelity simulator for autonomous driving. *arXiv preprint arXiv:2005.03778*.
- SAE On-Road Automated Vehicle Standards Committee. (2014) Taxonomy and definitions for terms related to on-road motor vehicle automated driving systems. *SAE Standard J*, 3016, 1–16.
- Sell, R., Coatanéa, E. & Christophe, F. (2008) Important aspects of early design in mechatronic. In *6th International Conference of DAAAM Baltic Industrial Engineering*, Tallinn.
- Sell, R., Leier, M., Rassölklin, A. & Ernits, J.-P. (2018) Self-driving car iseauto for research and education. In *2018 19th International Conference on Research and Education in Mechatronics (REM)* (pp. 111–116). Delft, Netherlands: IEEE.
- Sell, R., Rassölklin, A., Wang, R. & Otto, T. (2019) Integration of autonomous vehicles and industry 4.0. *Proceedings of the Estonian Academy of Sciences*, 68(4), 389–394.
- Sell, R., Soe, R.-M., Wang, R. & Rassölklin, A. (2020) Autonomous vehicle shuttle in smart city testbed. In *International Forum on Advanced Microsystems for Automotive Applications* (pp. 143–157). Springer.
- Shao, X., Liu, J. & Wang, H. (2018) Robust back-stepping output feedback trajectory tracking for quadrotors via extended state observer and sigmoid tracking differentiator. *Mechanical Systems and Signal Processing*, 104, 631–647.
- Shinpei, K. (2017) Autoware: ROS-based OSS for urban self-driving mobility. In *ROSCon Vancouver*. 2017. Open Robotics.
- Shufeng, W. & Junxin, Z. (2018) A research on overtaking lane planning for intelligent vehicles based on improved artificial potential field method. *Automobile Technology*, 3(2), 2–7.
- Silva, J. A. & Grassi, V. (2018) Clothoid-based global path planning for autonomous vehicles in urban scenarios. In *2018 IEEE International Conference on Robotics and Automation (ICRA)* (pp. 4312–4318). IEEE.
- Viana, I. B., Kanchwala, H. & Aouf, N. (2019) Cooperative trajectory planning for autonomous driving using nonlinear model predictive control. In *2019 IEEE International Conference on Connected Vehicles and Expo (ICCVE)* (pp. 1–6). Graz, Austria: IEEE.
- Wahde, M. (2008) *Biologically inspired optimization methods: an introduction*. WIT Press.
- Wahid, N., Zamzuri, H., Amer, N. H., Dwijotomo, A., Saruchi, S. A. & Mazlan, S. A. (2020) Vehicle collision avoidance motion planning strategy using artificial potential field with adaptive multi-speed scheduler. *IET Intelligent Transport Systems*, 14(10), 1200–1209.
- Wang, P., Gao, S., Li, L., Sun, B. & Cheng, S. (2019) Obstacle avoidance path planning design for autonomous driving vehicles based on an improved artificial potential field algorithm. *Energies*, 12(12), 2342.
- Xie, S., Hu, J., Ding, Z. & Arvin, F. (2021) Collaborative overtaking of multi-vehicle systems in dynamic environments: a distributed artificial potential field approach. In *2021 20th International Conference on Advanced Robotics (ICAR)*.
- Zhu, S., Gelbal, S. Y. & Aksun-Guvenc, B. (2018) Online quintic path planning of minimum curvature variation with application in collision avoidance. In *2018 21st International Conference on Intelligent Transportation Systems (ITSC)* (pp. 669–676). Maui, HI, USA: IEEE.

How to cite this article: Malayjerdi, E., Sell, R., Malayjerdi, M., Udal, A. & Bellone, M. (2022) Practical path planning techniques in overtaking for autonomous shuttles. *Journal of Field Robotics*, 39, 410–425.

<https://doi.org/10.1002/rob.22057>